Supplementary Figures

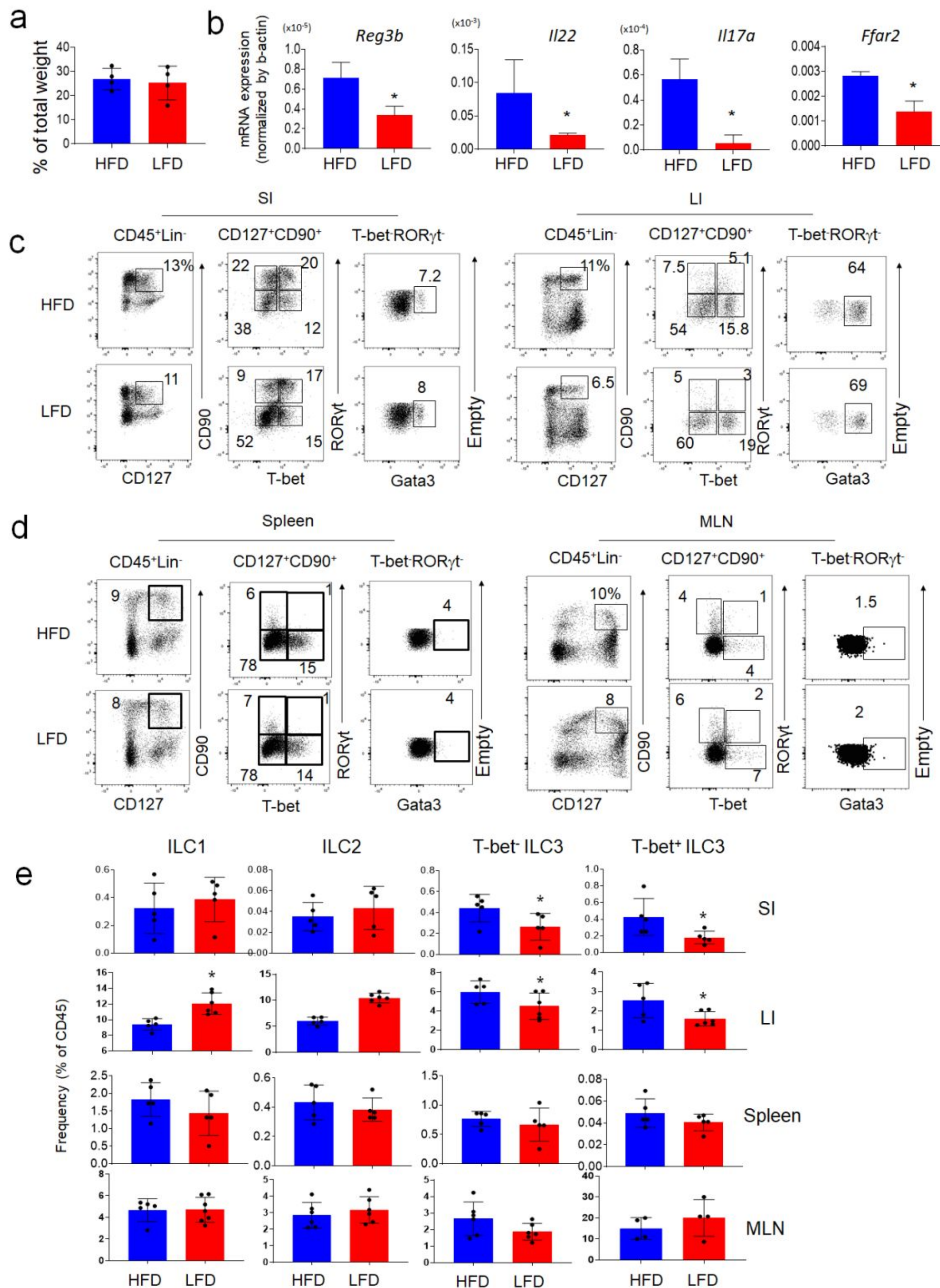

Figure S1. Effects of soluble DFs on ILCs in WT C57BL/6 mice. WT C57BL/6 mice were fed LFD or HFD and then infected with *C. rodentium* 3 week later. Two weeks later after infection, fecal water content (a), tissue mRNA expression of selected genes in colon tissues (b), ILC frequencies in various tissues (c-e) were determined. Representative and pooled data obtained from at least 2 different experiments (n=4-5) are shown. *Significant differences ($p<0.05$, 2-tailed T-test for panel b; 1-tailed t-test for panel e) between groups.

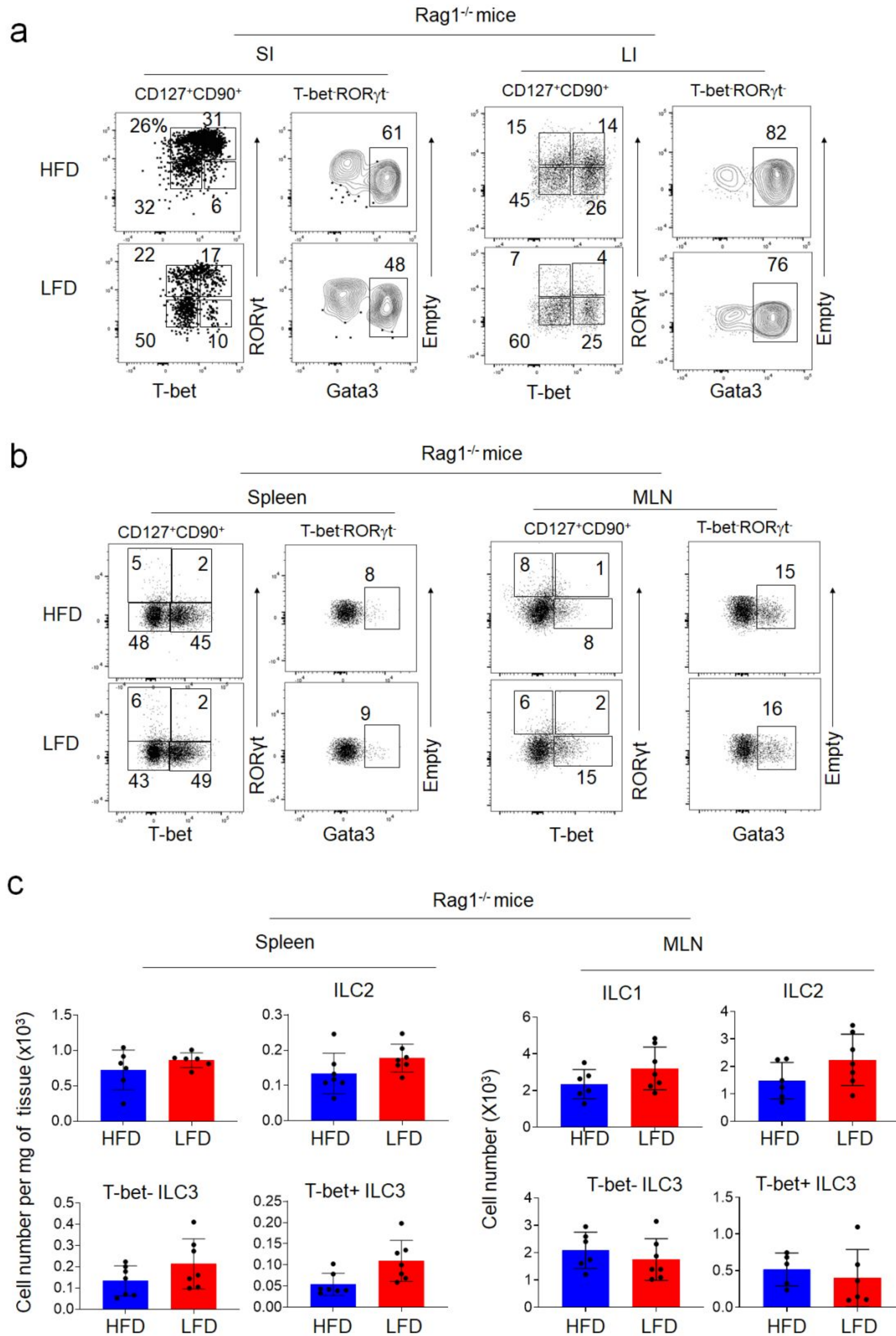

Figure S2. Effects of soluble DFs on ILC subsets in *Rag1*$^{-/-}$ mice. Mice were fed LFD or HFD from day 1 and infected with *C. rodentium* at the fourth week. Two weeks later, mice were compared for ILC numbers in various tissues. Representative flow data (a,b) and combined data (c) are shown. Representative and pooled data obtained from at least 2 different experiments (n=4-7) are shown. Significant differences ($p<0.05$) between groups.

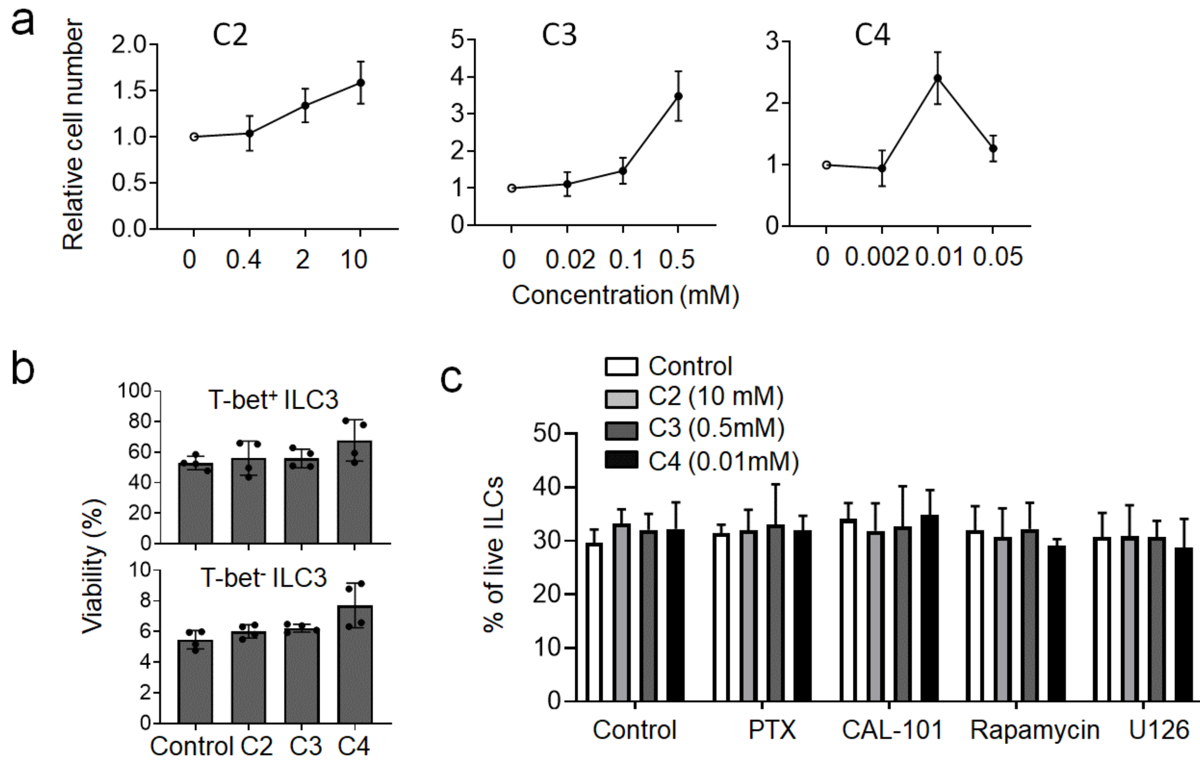

Figure S3. Effects of SCFAs on ILC proliferation (a) and survival (b). Splenocytes from *Rag1*$^{-/-}$ mice were cultured for 4 days in the presence of IL-23, IL-7, and IL-1β. SCFAs were added at indicated concentrations in panel a or 10 mM for C2, 0.5 mM for C3, and 0.01 mM for C4 in panel b. **(c) Effects of signaling inhibitors on ILC survival**. Inhibitors, such as U0126 (1 µM), rapamycin (25 nM), and CAL 101 (200 nM), were added to culture. Live and dead cells, based on Ghost dye Violet 450 staining, were counted by flow cytometry. Combined data are shown (n=3). Significant differences ($p<0.05$) between groups.

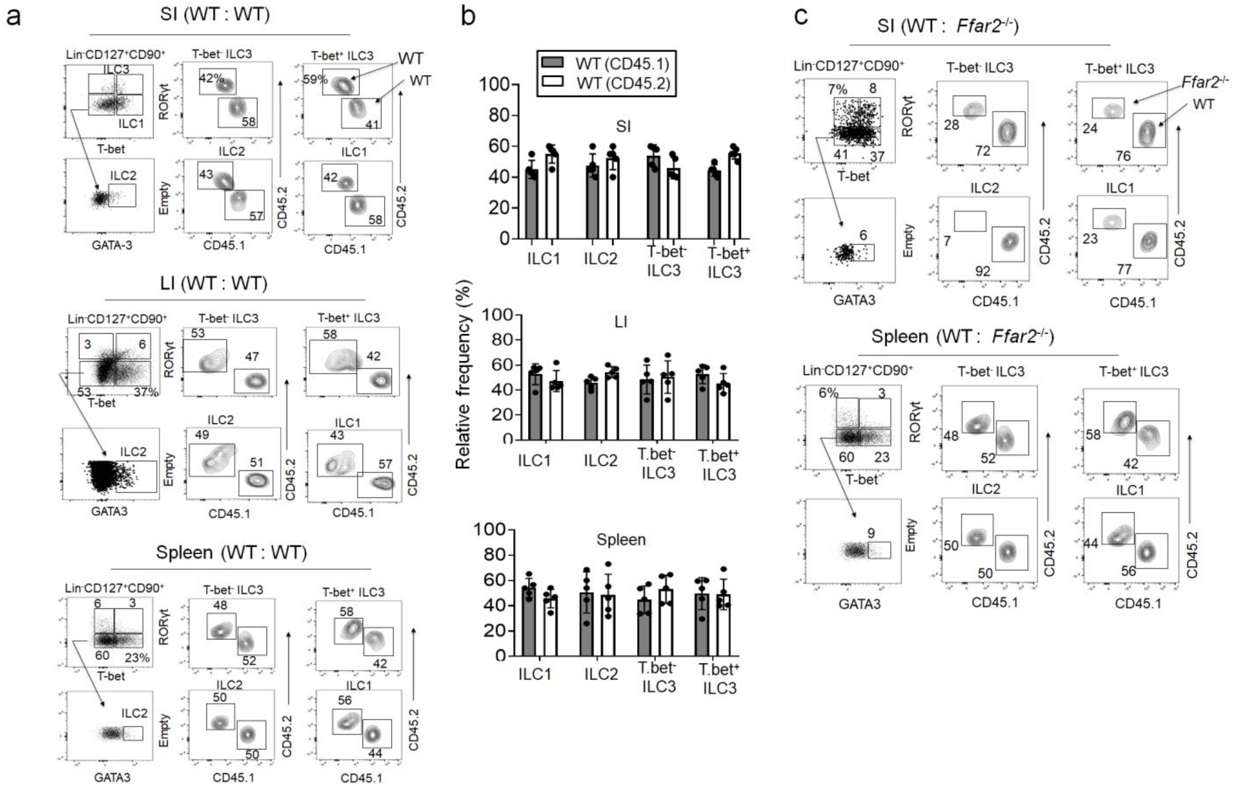

Figure S4. Competitive tissue population of WT and WT or *Ffar2$^{-/-}$* ILCs in *Rag2$^{-/-}$IL2R$\gamma^{-/-}$* mice. CD45.1$^+$ WT and CD45.2$^+$ WT (a,b) or CD45.2$^+$ *Ffar2$^{-/-}$* (c) Lin$^-$CD127$^+$ cells, isolated from spleen tissues, were co-transferred into *Rag2$^{-/-}$IL2R$\gamma^{-/-}$* mice. Mice were euthanized 4-5 weeks later, and ILC subsets were examined. Representative data obtained from at least 3 different experiments (n=5-9) are shown.

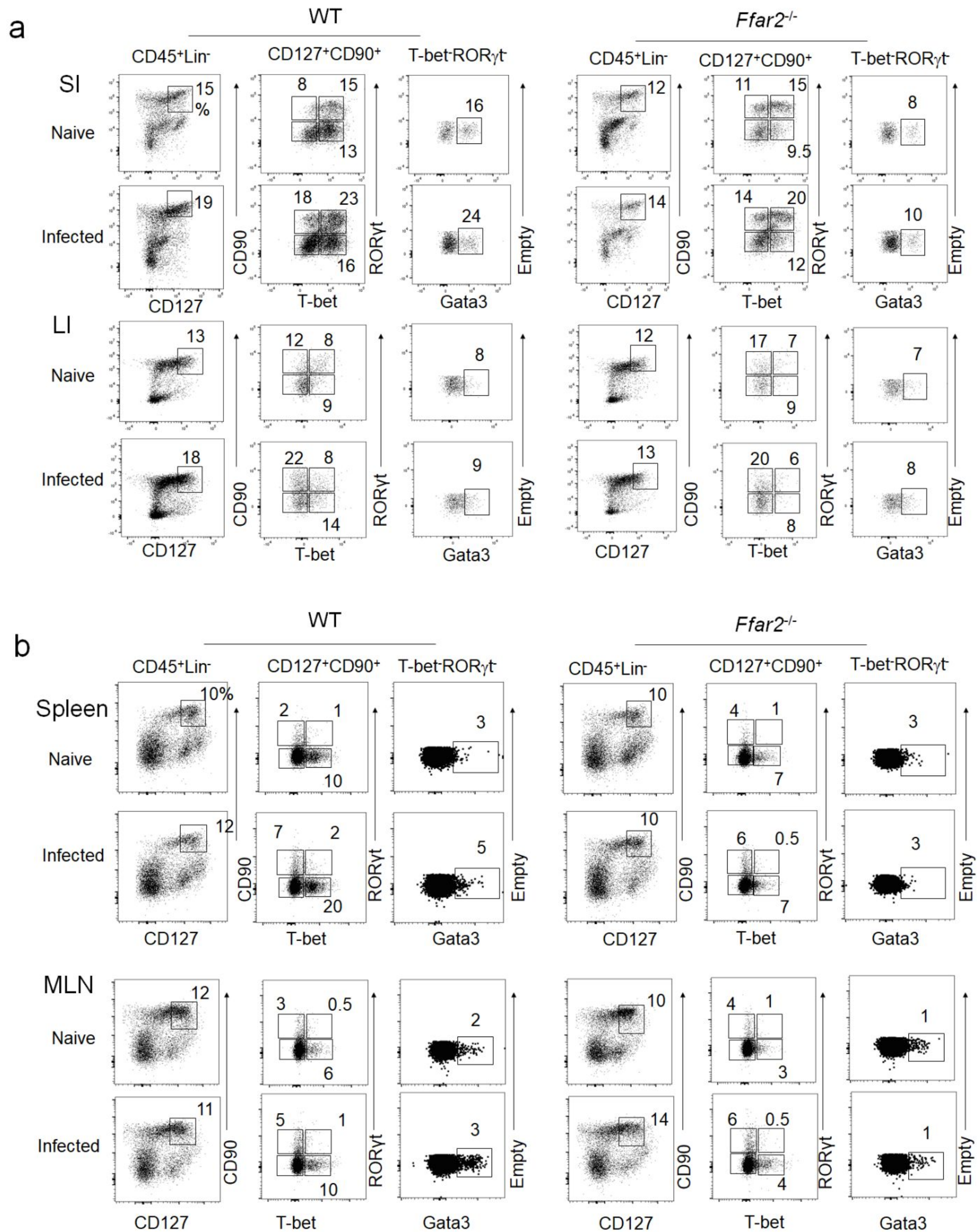

Figure S5. Tissue population of ILCs in *Ffar2*$^{-/-}$ mice following enteric bacterial infection. (a) WT and *Ffar2*$^{-/-}$ mice were infected with *C. rodentium* and examined by flow cytometry for ILC subsets in the intestines on day 14 post-infection. (b) ILC subsets in the spleen and MLN are shown. Representative data obtained from at least 3 different experiments (n=5-9) are shown.

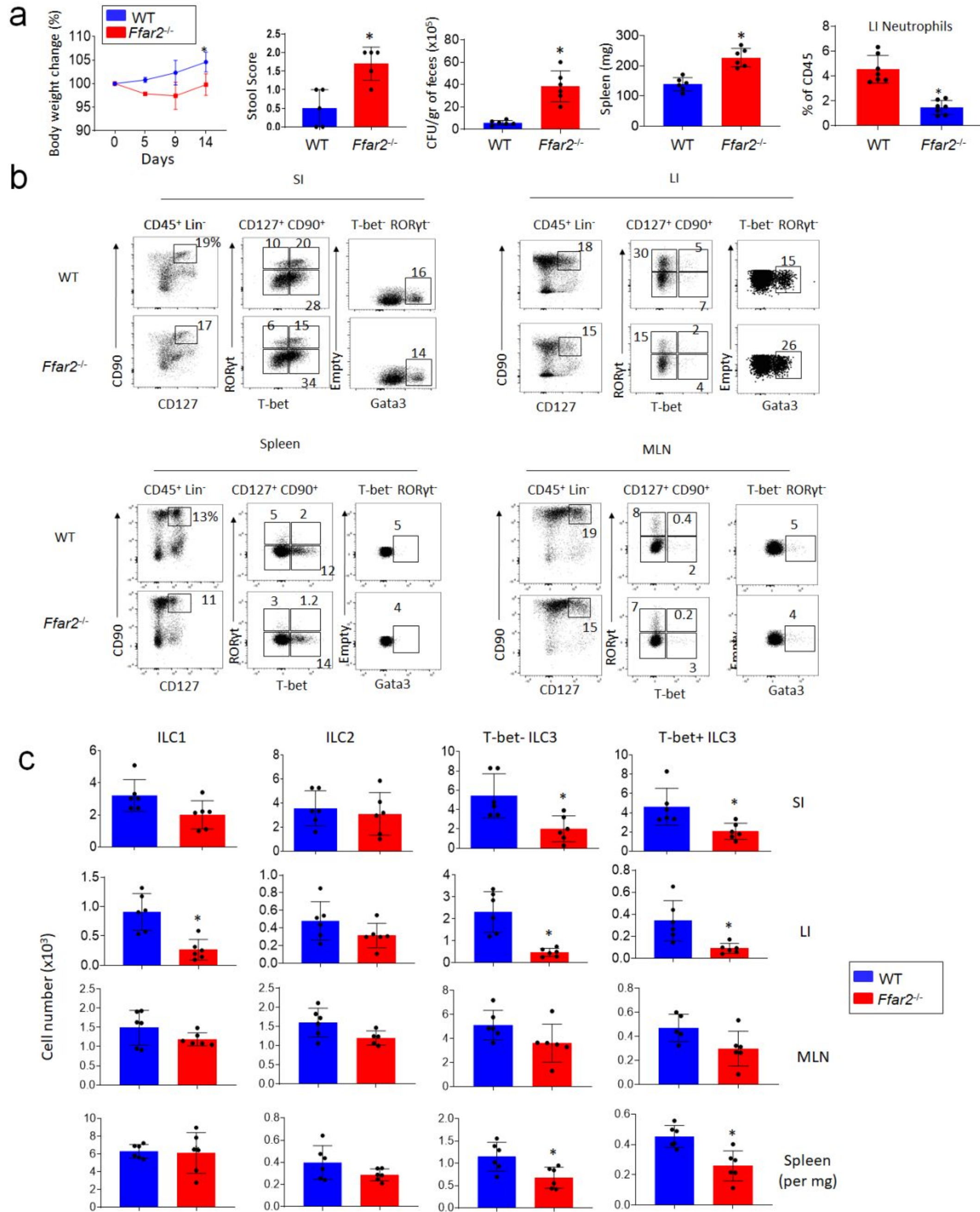

Figure S6. ILC responses in co-housed WT and *Ffar2*$^{-/-}$ mice. WT and *Ffar2*$^{-/-}$ mice were co-housed from 2-3 weeks before infected with *C. rodentium*. Mice were sacrificed 2 weeks after the infection. (a) Body weight change, pathogen burden per gram of feces, and spleen weight. (b, c) ILC subsets in indicated organs harvested on day 14 post-infection. Pooled data were obtained from 2 different experiments (n=6-7 per group) are shown. *Significant differences ($p<0.05$, one-tailed t-test) from WT.

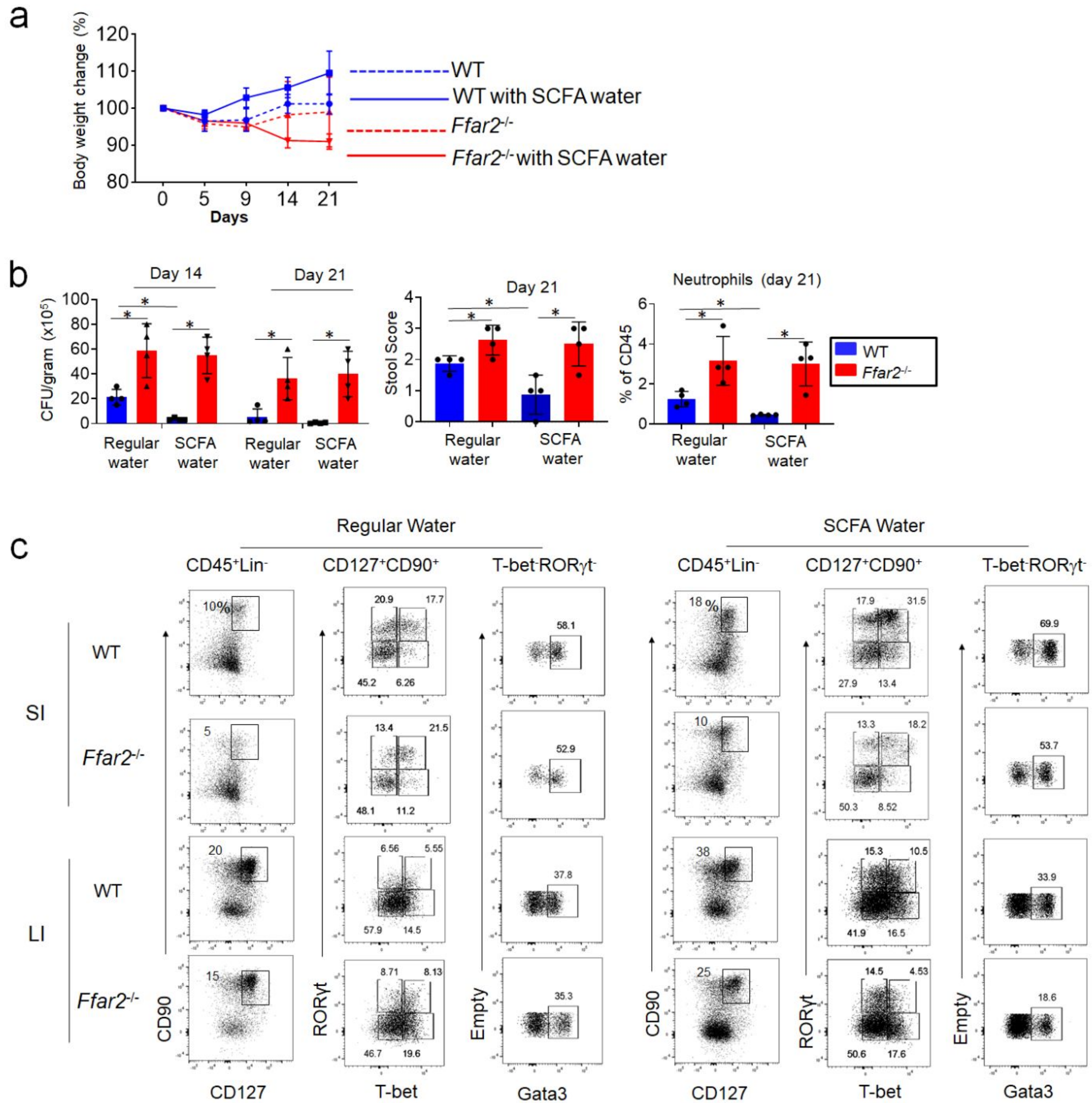

Figure S7. Effects of SCFAs on ILC numbers in WT versus Ffar2-deficient mice. WT and *Ffar2*$^{-/-}$ mice were fed LFD (no soluble fiber, 10% cellulose) and then with SCFAs in drinking water 2 weeks later. One week later, the mice were infected with *C. rodentium*. Two and three weeks later, mice were euthanized and ILC numbers in indicated tissues were determined. (a) Body weight change following infection. (b) *C. rodentium* burden per gram of feces, stool score, and neutrophils among the colonic lamina propria cells. (c) Representative flow cytometry data for intestines. Pooled and representative data obtained from 4-6 different mice are shown. *Significant differences (p<0.05) from WT.

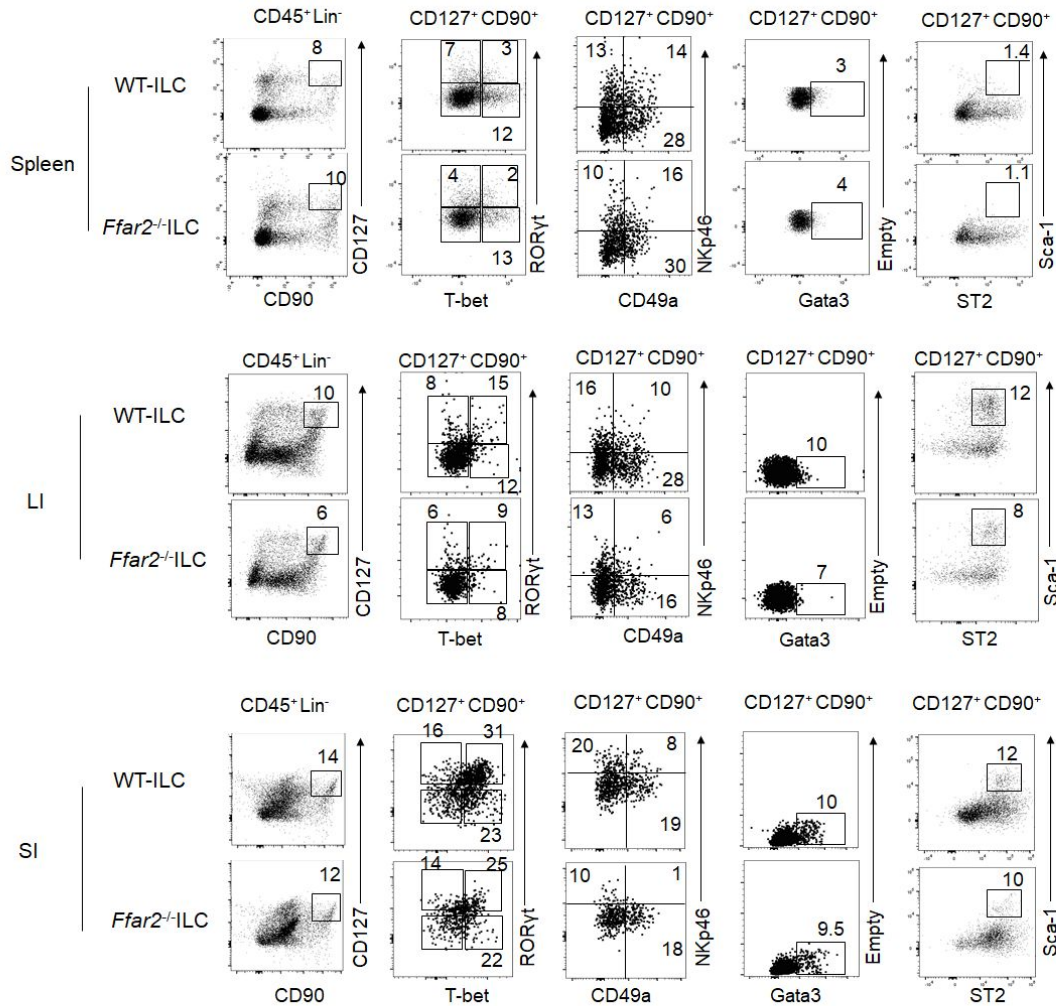

Figure S8. ILC responses in *Rag2*$^{-/-}$ *IL2Rγ*$^{-/-}$ mice following cell transfer with WT versus *Ffar2*$^{-/-}$ ILCs. WT and *Ffar2*$^{-/-}$ ILCs, isolated from spleen tissues, were separately transferred into *Rag2*$^{-/-}$*IL2Rγ*$^{-/-}$ mice. Three weeks later, these mice were infected with *C. rodentium*. Mice were sacrificed 8 days later and ILC populations were examined. Representative data obtained from 2 independent experiments (n=6 each group) are shown

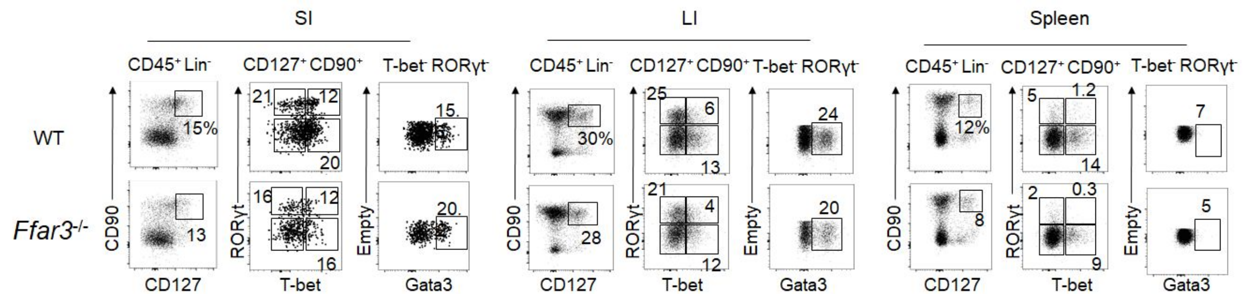

Figure S9. ILC responses in WT and *Ffar3*$^{-/-}$ mice WT and *Ffar3*$^{-/-}$ mice were infected with *C. rodentium* and examined by flow cytometry for ILC subsets on day 14 post-infection. Representative data obtained from 2 independent experiments (n=4-7 each group) are shown.

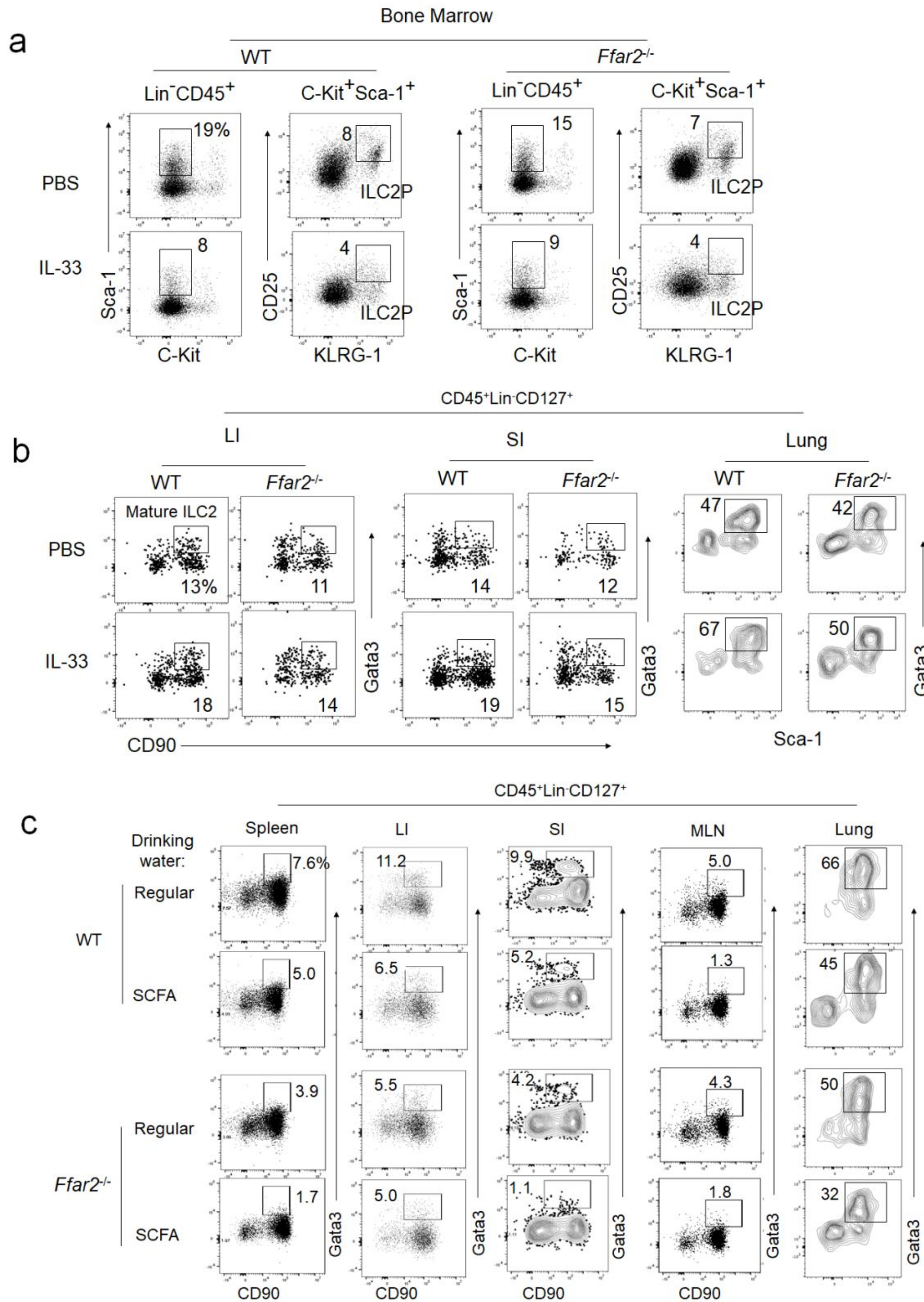

Figure S10. ILC2 response in *Ffar2$^{-/-}$* mice following IL-33 administration with or without oral administration of SCFAs. (a,b) WT and *Ffar2$^{-/-}$* mice were injected with IL-33 for three consecutive days, and ILC2P numbers in the bone marrow (a) and peripheral organs (b) were examined 36h later. For panel a and b, mice were kept on regular rodent chow. (c) A similar experiment was performed on mice fed LFD alone versus LFD and SCFA in drinking water. Mice were kept on LFD diet from 2 weeks prior to IL-33 injection (3 times). Representative data from 2 independent experiments are shown.

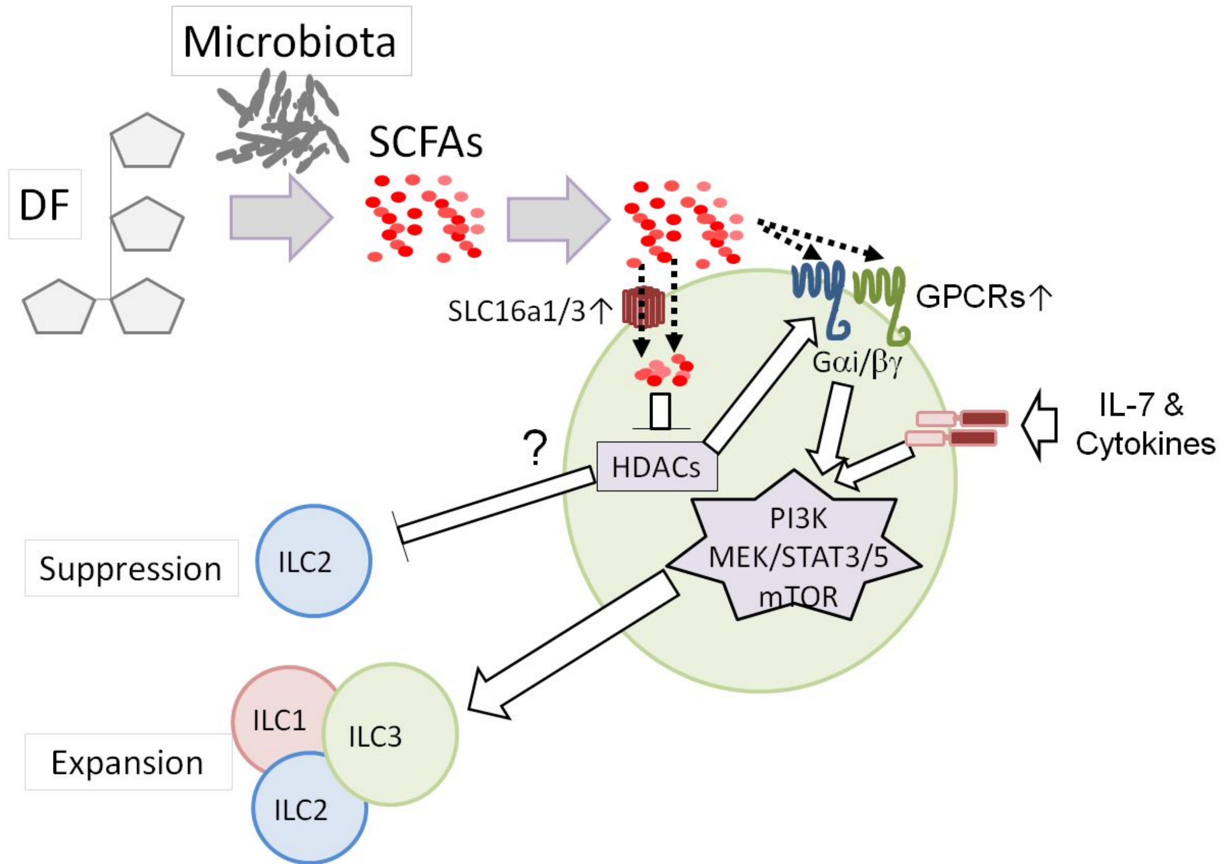

Figure S11. A model for the functions of SCFAs and GPCR signaling in regulation of ILCs. Our findings support the roles of SCFAs in supporting the peripheral expansion of ILC1, ILC2 and ILC3. This function is mediated by GPCR-mediated signaling that boosts cytokine (e.g. IL-7)-induced cell signaling, such as PI3K, MEK, mTOR, STAT3, and STAT5, leading to ILC population expansion. While GPCRs enhance the expansion of ILC1, ILC2 and ILC3, SCFAs have the potential to negatively regulate ILC2. The negative regulation may be mediated by other mechanisms, such as HDAC inhibition and/or indirect regulation through other cell types.